

Maltase Decorated by Chiral Carbon Dots with Inhibited Enzyme Activity for Glucose Level Control

Mengling Zhang, Huibo Wang, Bo Wang, Yurong Ma, Hui Huang, Yang Liu,*
Mingwang Shao,* Bowen Yao,* and Zhenhui Kang*

Carbon dots (CDs) have attracted increasing attention in disease therapy owing to their low toxicity and good biocompatibility. Their therapeutic effect strongly depends on the CDs structure (e.g., size or functional groups). However, the impact of CDs chirality on maltase and blood glucose level has not yet been fully emphasized and studied. Moreover, in previous reports, chiral CDs with targeted optical activity have to be synthesized from precursors of corresponding optical rotation, severely limiting chiral CDs design. Here, chiral CDs with optical rotation opposite to that of the precursor are facily prepared through electrochemical polymerization. Interestingly, their chirality can be regulated by simply adjusting reaction time. At last, the resultant (+)-DCDs ($700 \mu\text{g mL}^{-1}$) are employed to modify maltase in an effort to regulate the hydrolytic rate of maltose, showing an excellent inhibition ratio to maltase of 54.7%, significantly higher than that of (–)-LCDs (15.5%) in the same reaction conditions. The superior performance may be attributed to the preferable combination of DCDs with maltase. This study provides an electrochemical method to facily regulate CDs chirality, and explore new applications of chiral CDs as antihyperglycemic therapy for controlling blood glucose levels.

Nowadays, diseases arisen from high blood glucose level have grown explosively around the world, including type 2 diabetes, hyperglycemia, and some cardiovascular diseases.^[1,2] Besides, a high blood glucose level also severely endangers those people with impaired glucose tolerance^[3,4] Therefore, controlling blood glucose level is critical in the process of therapy. There are several types of oral antihyperglycemic drug for decreasing blood glucose level, such as biguanides, sulfonylureas, and α -glucosidase inhibitor. Among these medicines, biguanides and sulfonylureas can efficiently decrease high blood glucose but usually accompanied by serious side effects,^[5,6] whereas α -glucosidase inhibitors (e.g., acarbose and miglitol) are safer

but with a lower efficacy than biguanides and sulfonylureas.^[3,5,7] Therefore, it is necessary to develop a new inhibitor with a high inhibitory efficacy for antihyperglycemic.

Carbon dots (CDs), as an emerging subclass of carbon materials, having been applied in various biological applications, including bioimaging, drug/gene delivery, antimicrobial and plant biology, owing to their low toxicity, well biocompatibility, and biodegradable property.^[8–10] For different purpose, CDs have been reported to combine with various drug or biomacromolecules, such as (1) CDs/protoporphyrin IX composite for nucleolus imaging and nucleus-targeted drug delivery owing to their selectively targeting nucleolus ability^[11]; (2) CDs/ssDNA composite as ideal fluorescent sensing platform for nucleic acid detection^[12]; (3) In addition, CDs can be biodegraded to plant hormone analogues and CO_2 through the horseradish peroxidase of plants, demonstrating its excellent biocompatibility.^[13]

Chirality is a common phenomenon, and takes critical role in physiological activities.^[14,15] Therefore, the CDs chirality are also expected to strongly affect their biological properties. For instance, L-CDs prepared from L-cysteine showed upregulated glycolysis in cellular energy metabolism of human bladder cancer T24 cells, but D-CDs showed no effect^[16]; L-CDs synthesized from L-lysine dramatically remodeled A β 42 structure and inhibited A β 42 cytotoxicity, compared with D-CDs^[17]; D-CDs obtained from D-glutamic acid have more efficient antimicrobial activity towards both Gram-negative and Gram-positive bacteria than L-CDs^[18]; Besides, the different chirality of CDs can even showed opposite effects. For example, the L-CDs synthesized from L-cysteine can improve laccase activity, whereas its counterpart D-CDs impair the activity.^[19] However, the effect of chiral CD on maltase and blood glucose level was rarely reported. Besides, according to the previous reports, chiral CDs of targeted optical activity have to be synthesized from precursor of corresponding optical rotation (e.g., L-CDs must be prepared from sinistral precursor), severely limiting the strategies to synthesize chiral CDs. Chiral CDs with optical rotation opposite to that of precursor have barely been reported.

Herein, chiral CDs were prepared by electrochemical polymerization from L- or D-glutamic acid (Glu) in aqueous alkali, and

M. Zhang, H. Wang, B. Wang, Y. Ma, Prof. H. Huang, Prof. Y. Liu,
Prof. M. Shao, Dr. B. Yao, Prof. Z. Kang
Institute of Functional Nano & Soft Materials (FUNSOM)
Jiangsu Key Laboratory for Carbon-Based Functional Materials & Devices
Soochow University
199 Ren'ai Road, Jiangsu, Suzhou 215123, P. R. China
E-mail: yangl@suda.edu.cn; mwshao@suda.edu.cn; bw Yao@suda.edu.cn;
zhkang@suda.edu.cn

 The ORCID identification number(s) for the author(s) of this article can be found under <https://doi.org/10.1002/sml.201901512>.

DOI: 10.1002/sml.201901512

their optical activity was tuned facilely by controlling the operating time of preparation. Interestingly, the circular dichroism (CD) optical orientation could even transform (e.g., from sinistral to dextral) after simply prolonging the reaction times to 6 d. Finally, their inhibitory efficiencies on maltase activity were studied in terms of inhibition ratio and Michaelis constant (K_m and V_{max}) by using maltase and maltase/CDs hybrids as enzyme and maltose as substrate. The superior performance may be attributed to the preferable combination of DCDs with maltase. To sum up, this study provides a new method to regulate CDs chirality, and develop chiral CDs as antihyperglycemic therapy for controlling blood glucose level.

The chiral CDs were synthesized by electrochemical polymerization from L- or D-Glu in aqueous alkali (Figure 1). Considering the low solubility of L- or D-Glu in water solution, the pH of the solution was increased by adding NaOH to enhance their solubility and increase the electrical conductivity of electrolyte during the electrochemical synthesis.^[19] The chiral CDs ((+)-LCDs or (-)-DCDs) could be obtained after 3 d and their optical activity were inherited from L-(+) or D-(-)-Glu. Interestingly, the optical activity of CDs was reversed after electropolymerization for 6 d. When L-(+)-Glu or D-(-)-Glu were used as precursor, (-)-LCDs or (+)-DCDs (hereinafter called as LCDs and DCDs) were obtained. The text mainly discussed DCDs and the characterization of LCDs are provided in the Supporting Information.

The morphologies of chiral CDs were obtained by transmission electron microscopy (TEM) and atomic force microscopy (AFM). As shown in Figure 2a, DCDs were well dispersed, and their diameter ranged from 2 to 6 nm. The high-resolution transmission electron microscopy (HRTEM, the inset of Figure 2a) revealed the lattice spacing of 0.21 nm, corresponding to the (100) crystal facet of graphite.^[20] As shown in AFM images, DCDs had a circle shape with the topographic height of 3–7 nm (Figure S1, Supporting Information), agreeing well with the results of TEM characterization. The AFM and TEM images of LCDs were shown in Figures S1 and S2 in the Supporting Information.

The elementary composition and chemical structures of CDs were analyzed by X-ray photoelectron spectroscopy (XPS) and Fourier transform infrared (FTIR) spectrum. The full scan XPS spectrum of DCDs and LCDs were shown in Figures S3a and S4a (Supporting Information), which showed the CDs were mainly composed by C, N, and O elements. For DCDs, C, N, and O accounted for 58.40, 7.49, and 34.11 at%. The C 1s XPS spectrum of DCDs (Figure 2b) could be deconvoluted into three peaks at 284.60, 286.00, and 287.80 eV, corresponding with C–C, C–O/C–N, and C=O.^[21,22] One surface components of DCDs could be found in the N1s deconvoluted spectra and the peak at 399.50 eV was belonged to the pyridinic N (Figure S3b, Supporting Information).^[21,23] The analysis results of XPS for LCDs were displayed in Figure S4 in the Supporting Information. The FTIR spectrum was employed for analyzing the surface functional groups of the obtained chiral CDs (Figure 2c). The vibrational absorption signals were less than raw materials (black line). The peak at 3446 cm^{-1} was corresponded to the stretching vibration of O–H or N–H.^[24] The vibrational absorption signals at 1578 and 1390 cm^{-1} could be attributed to the vibration of C=C and C–O.^[21,25] Furthermore, FTIR spectrum of LCDs (blue line) and DCDs (red line) showed similar functional groups, such as –NH and –OH.

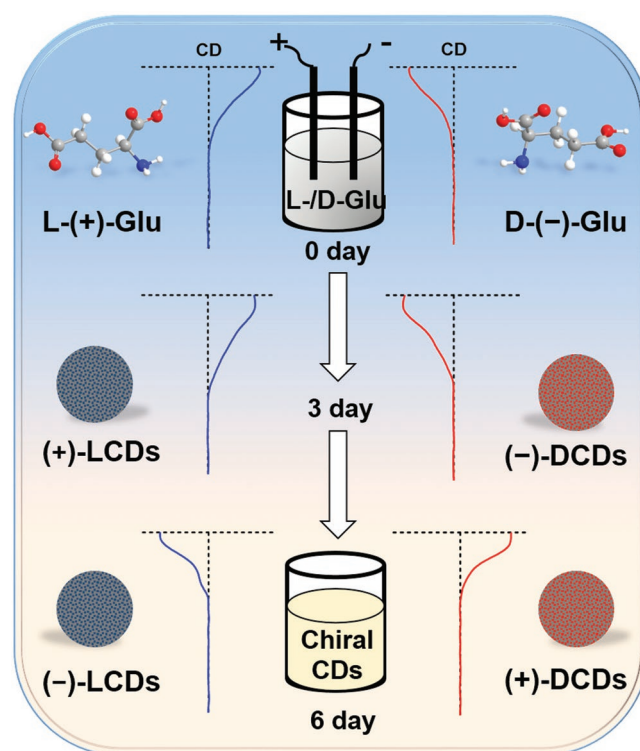


Figure 1. Schematic for the synthesis of chiral CDs.

UV–vis absorption spectrum, photoluminescence (PL) spectrum, and CD spectrum were measured to study the optical properties of chiral CDs. For the UV–vis absorption of L-Glu (Figure S5, black line, Supporting Information), only one absorption peak located at 208 nm was observed in the absorption curve, which corresponded to $\pi-\pi^*$ transitions.^[26] After CDs were formed, the $\pi-\pi^*$ transitions showed a red shift from 208 to 218 nm as the result from the expanded conjugated domains,^[27] and a new $n-\pi^*$ transitions (the peak located at 283 nm) appeared (Figure 2d, black line; and Figure S5, blue line, Supporting Information).^[26,28] PL spectrum of chiral CDs was also detected (Figure 2d; Figure S6, Supporting Information). DCDs solution revealed an optimal emission at 405 nm (Figure 2d, red line) with 325 nm excitation (Figure 2d, blue line). The CD spectrums of chiral CDs were also measured for monitoring the formation of CD chirality. As illustrated in Figure 2e, the chiral signals of CDs prepared at different electrolysis time were measured. When the solution was electrolyzed for 1 d, the CD signal located at 205 nm. With the electrolysis time increased to 2 d, the intensity of CD signal at 205 nm significantly increased. The CD signal of precursors (Figure S7, Supporting Information) was at 205 nm as well. Hence, the CD signal located at 205 nm from chiral CDs should be inherited from L- or D-Glu. However, when the electrolysis time extended to 3 d, the intensity of CD signal decreased. Then, since the electrolysis time was prolonged to 4 d, the CD signal of solution disappeared. Interestingly, the signal does not vanish with the increase of electrolysis time to 5 and 6 d, but a reverse CD signal of the solution appeared at the same position and the intensity of this signal gradually increased. A pair of chiral CDs with opposite optical rotation to the raw materials was obtained

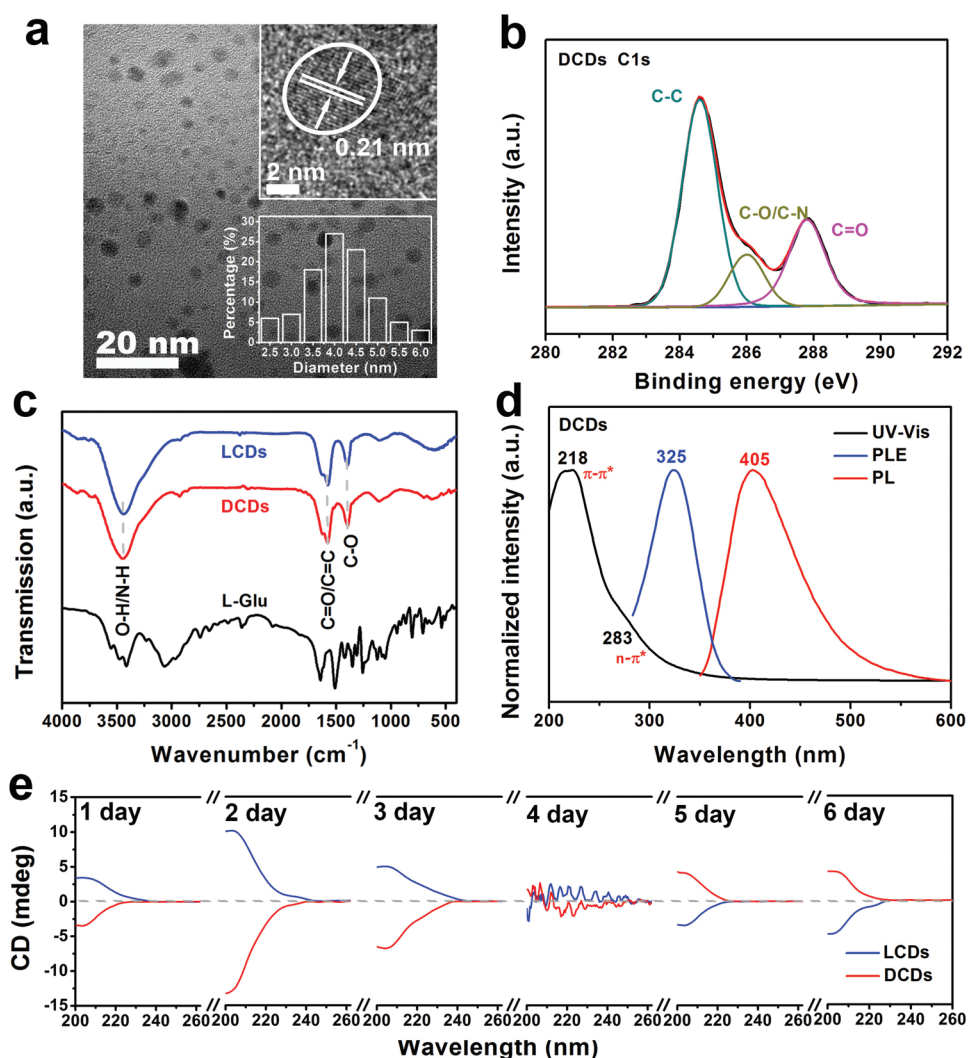


Figure 2. Characterization of CDs. a) TEM image and b) XPS spectrum of DCDs; c) The FTIR spectrum of LCDs (blue line), DCDs (red line), and L-Glu (black line); d) UV-vis spectrum (black line), PLE excitation (blue line), and emission spectrum (red line) of DCDs; e) The CD spectrum of LCDs (blue line) and DCDs (red line) prepared at 1–6 d, respectively.

through a facile alkaline-assisted electrochemical polymerization from L- and D-Glu.

Maltase is a key enzymes involved in carbohydrates digestion and it can catalyzes the hydrolysis of maltose to the blood glucose in human body.^[7,29] Controlling blood sugar level has attract the attention of researchers with the improving of living standard.^[1] Before biological application of the chiral CDs, the cytotoxicity and biocompatibility of chiral CDs was evaluated via 293T cells at first, which was incubated with CDs with an increasing concentration. As shown in Figure S8 (Supporting Information), the chiral CDs did not affect the growth and proliferation of the 293T cells even at an ultrahigh concentration (2.4 mg mL^{-1}). This data demonstrated the chiral CDs were low toxicity and benign biocompatibility.

In the following experiment, the chiral CDs with opposite optical rotation to the raw materials were combined with maltase for tuning activity. **Figure 3a** showed the glucose concentration versus different reaction times for maltase (black line), maltase/LCDs (blue line), and maltase/DCDs (red line).

The concentration of maltase and LCDs or DCDs were 3.6 mg mL^{-1} and $700 \text{ } \mu\text{g mL}^{-1}$. Throughout the first 30 min after the reaction started, the glucose generation rate was proportional to the reaction time. When the reaction time reached to 90 min, the enzymatic reaction reached equilibrium. During 3 h of the reaction, it was obvious that both the LCDs and DCDs inhibited the activity of maltase and the DCDs had better inhibitory effect than the LCDs. For better understanding the influence of different concentration of chiral CDs in the catalytic activity of maltase/LCDs or maltase/DCDs, the inhibition ratio of chiral CDs with different concentration ($200, 400, 700, 1000, 1500 \text{ } \mu\text{g mL}^{-1}$) were detected (Figure 3b) when the reaction reached equilibrium (90 min). With the increasing concentration, the inhibition ratio of maltase/LCDs (blue trace) and maltase/DCDs (red trace) gradually enhanced. Remarkably, in the concentration of CDs ranging from $200\text{--}1500 \text{ } \mu\text{g mL}^{-1}$ in maltase/LCDs or maltase/DCDs hybrids, DCDs had more effective in inhibiting the activity of maltase. That is to say, the chirality of the CDs had an impact on the activity of maltase.

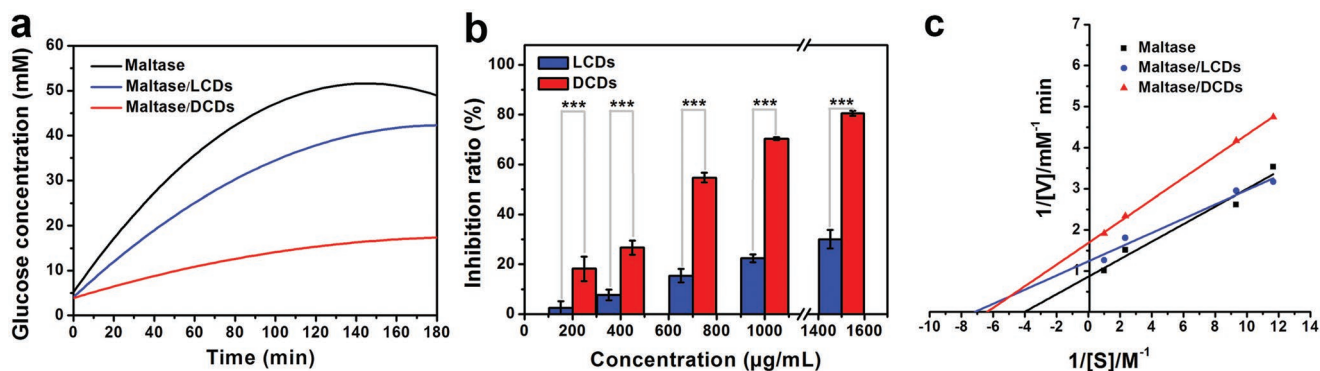


Figure 3. Maltase inhibitory activities of chiral CDs. a) The glucose concentration of the maltose degradation for maltase (black line), maltase/LCDs (blue line), and maltase/DCDs (red line) at different hydrolysis times (0–180 min, the concentration of maltase and LCDs or DCDs is 3.6 mg mL⁻¹ and 700 μg mL⁻¹, respectively); b) The inhibition ratio of LCDs (blue trace) and DCDs (red trace) with different concentration (200–1500 μg mL⁻¹) after 90 min reaction (maltase: 3.6 mg mL⁻¹); c) Lineweaver–Burk plots of maltase (black line), maltase/LCDs (blue line), and maltase/DCDs (red line); (M: mol L⁻¹, m M: mmol L⁻¹, Mean ± SD, ****P* < 0.001).

To investigate how the chiral CDs inhibited the activity of maltase, Michaelis–Menten kinetics analysis was employed and the Michaelis constants (K_m and V_{max}) for maltase, maltase/LCDs, and maltase/DCDs were obtained by Lineweaver–Burk plot. K_m and V_{max} could be calculated from the ordinate and abscissa intercept which represent the value of $1/V_{max}$ and $-1/K_m$.^[30,31] The Lineweaver–Burk plot of maltase (black line), maltase/LCDs (blue line), and maltase/DCDs (red line) were shown in Figure 3c and the value of Michaelis constants were shown in Table S1 in the Supporting Information. The concentration of maltase and LCDs or DCDs were 3.6 mg mL⁻¹ and 700 μg mL⁻¹. From the Lineweaver–Burk plot, the value of the V_{max} of maltase, maltase/LCDs, and maltase/DCDs were 1.16, 0.80, and 0.59 mmol L⁻¹ min⁻¹ and the K_m of which were 0.25, 0.13, and 0.17 mol L⁻¹, respectively. In the same reaction conditions, both the V_{max} and K_m of maltase/LCDs or maltase/DCDs decreased, which demonstrated the LCDs or DCDs was a kind of mixed inhibitor for maltase.^[31,32] Besides, comparing maltase/LCDs with maltase/DCDs, the V_{max} of maltase/LCDs was greater than maltase/DCDs in the maltase concentration of 3.6 mg mL⁻¹, indicating the maltase/LCDs had higher catalytic efficiency than maltase/DCDs. For K_m , which value is equal to the concentration of substrate when the reaction rate reach to the half of V_{max} .^[31] In spite of the smaller V_{max} of maltase/DCDs compared with maltase/LCDs, the K_m of maltase/DCDs were larger than that of maltase/LCDs. It demonstrated the weaker affinity of maltase/DCDs towards the maltose. Taking the above discussions into consideration, the maltase/DCDs had the higher inhibitory effect than maltase/LCDs hybrids.

To better confirm the combination of LCDs or DCDs with maltase. Sodium dodecyl sulfate polyacrylamide gel electrophoresis (SDS-PAGE) test, dynamic light scattering (DLS) detection, CD spectrum, and PL spectrum for maltase and maltase/CDs hybrids were analyzed. The result of SDS-PAGE test was shown in Figure 4a. The displacement distance of the maltase/LCDs is shorter than free maltase, and the maltase/DCDs was slower than maltase/LCDs and free maltase, which demonstrated that the LCDs or DCDs successfully combined with maltase and the DCDs combined more effectively with maltase than the LCDs. For further demonstrating the successful combination, DLS

was used for testing the hydrodynamic diameter of maltase (black line) and maltase/CDs hybrids (maltase/LCDs: blue line; maltase/DCDs: red line). As shown in Figure 4b, the size of maltase/CDs hybrids were larger than free maltase. In the hydrodynamic diameter of maltase/LCDs and maltase/DCDs, it was more change in the size of the maltase/DCDs than which of the maltase/LCDs. From the discussion above, it could be confirmed that the chiral CDs could be combined with maltase. For investigating the interaction between maltase and chiral CDs in maltase/CDs hybrids, PL spectrums of maltase (black line), maltase/LCDs (blue line) and maltase/DCDs (red line) were obtained (Figure 4c). The fluorescence intensity of maltase/CDs is higher than free maltase and the emission peak is almost unchanged (about 7 nm), illustrating the chiral CDs may be combined with maltase by noncovalent bonds.^[30] Then, the secondary structure of maltase and maltase/CDs hybrids were analyzed by CD spectrum (Figure 4d), compared with the CD signals of free maltase (black line), the intensity of CD signals of the maltase/LCDs (blue line) and maltase/DCDs (red line) decreased at the negative peaks of 208, 222 nm (α -helix), and 218 nm (β -helices).^[33,34] However, the intensity of CD signals for maltase/DCDs was lower than that of the maltase/LCDs hybrid, suggesting that the chiral CDs had changed the structure of maltase and the structure of maltase treated with DCDs changed more. Based on the above discussion, the possible inhibition mechanism of chiral CDs for Maltose catalyzed reaction might be as follows: the chiral CDs could be combined with maltase by noncovalent bonds and then changed the structure of maltase. They may occupy the active sites or other sites of maltase. And then, the maltase/CDs hybrids likely hindered the combination of enzyme with substrates for reducing enzymatic activity. Another possibility is that the maltase/CDs hybrids could combine with substrates to form a maltase/CDs/maltose compound, which could not release the products resulted in the low glucose content. Besides, the DCDs could be preferably combined with maltase and affected its activity compared with the LCDs.

In summary, we have prepared chiral CDs by electrochemical polymerization from L-(+)- and D-(-)-Glu in aqueous alkali. The chirality of CDs could be regulated and even reversed by controlling reaction time. With the increase of electrolysis time, the

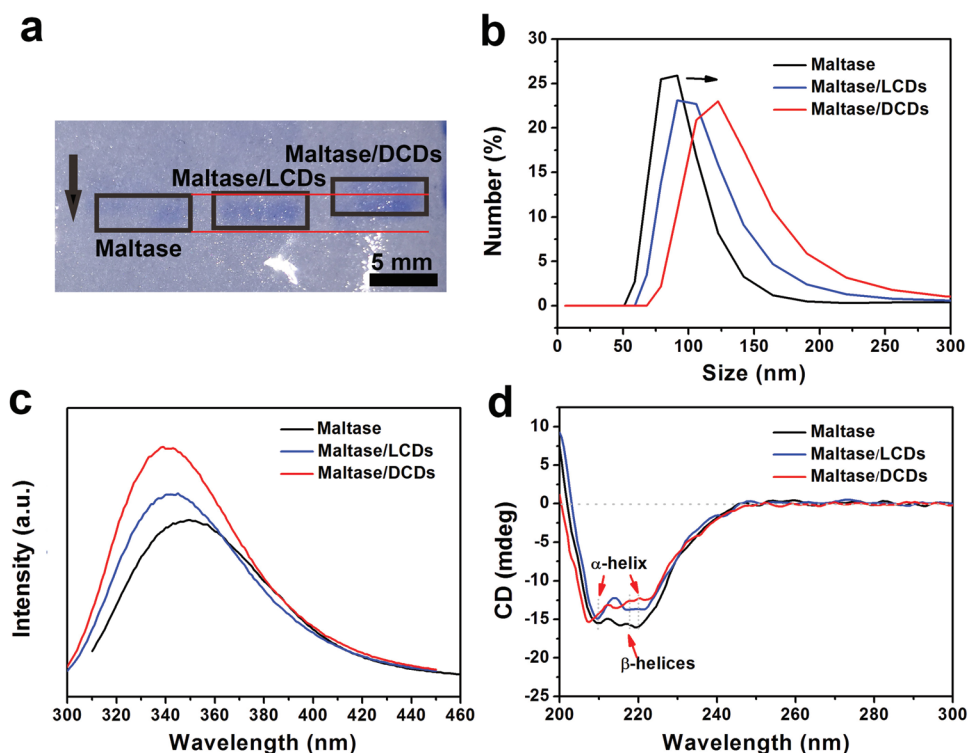


Figure 4. The combination of LCDs or DCDs with maltase. a) The SDS-PAGE, b) hydrodynamic diameter, c) PL spectrum ($\lambda_{\text{ex}} = 280 \text{ nm}$), and d) CD spectrum of the maltase (black line), maltase/LCDs (blue line), and maltase/DCDs (red line). The concentration of maltase and LCDs or DCDs was 2.5 and 1.5 mg mL^{-1} , respectively.

CD signal located at 205 nm increased first and then gradually decreased, and finally reversed at the same position. The chiral CDs with good biocompatibility could inhibit the activity of maltase. They could act as a mixed inhibitor to reduce the production of blood glucose. However, DCDs had higher inhibitory efficiency than LCDs, which was attributed to that the DCDs could preferably combined with maltase by noncovalent bonds and then changed the structure of maltase. In addition, compared with the maltase/LCDs hybrids, the maltase/DCDs had weaker affinity towards the substrate, which was manifested in the larger value of the Michaelis constants K_m of maltase/DCDs hybrid and the maltase/DCDs had a smaller V_{max} . We have provided a new method to regulate CDs chirality, and developed chiral CDs as antihyperglycemic therapy for controlling blood glucose level.

Experimental Section

Materials: L- or D-Glu and cellulose dialysis bag (500–1000 Da) were purchased from Shanghai Yuanye Biotechnology Co. Ltd. NaOH was purchased from Beijing Chemical Reagent (Beijing, China). D-(+)-maltose monohydrate was obtained from Shanghai Macklin Biochemical Technology Co. Ltd. Maltase was purchased from Dalian Meilune Biotechnology Co. Ltd. Glucose assay kit was purchased from Shanghai Rongsheng Biotech Co. Ltd. Cell Counting Kit-8 was obtained from Beyotime Biotechnology Co. Ltd. The graphite rod (99.99%) was obtained from Shanghai Carbon Co. Ltd. All chemicals were used without any further purification.

Synthesis of Chiral CDs: The chiral CDs were prepared by electrochemical polymerization. In brief, L- or D-Glu (3 g) and NaOH

(3 g) were dissolved in milli-Q water (300 mL). Then, two graphite rods as anode and cathode were inserted into the above solution, respectively. Constant current (0.02 A) was supplied by a DC power supply. After 6 d, the color of the solution changed from colorless to yellowish brown. For removing impurities, the reaction mixture was dialyzed against ultrapure water by a cellulose dialysis membrane (500–1000 Da) for 3 d. Finally, the chiral CDs (LCDs or DCDs) were obtained. In order to better monitor the formation of chiral CDs. The products were prepared at different time (1–6 d) in the above way and monitored their chiral signal.

Preparation of Maltase/CDs Hybrids: Maltase powder (0.05 g) was dissolved in phosphate buffer saline (PBS, 0.1 mol L^{-1} , 5 mL) sufficiently and the solution was centrifuged at 5000 rpm for 10 min to remove the insoluble part. Then, different concentrations (0–1500 $\mu\text{g mL}^{-1}$) of LCDs or DCDs were added into maltase solution (3.6 mg mL^{-1}) and the mixture was incubated at 37 °C for 6 h. Herein, the chiral CDs had been lyophilized and dissolved in PBS (0.1 mol L^{-1}).

Activity Assays of Maltase and Maltase/CDs Hybrids: In order to rule out the influence of other factors, during the preparation of maltase/CDs hybrids, the same concentration of maltase solution as control was incubated at 37 °C for 6 h as well. This experiment was repeated at least three times to ensure the accuracy of the results. Maltose (0.14 mol L^{-1}) as the substrate and maltase solution (3.6 mg mL^{-1}) was mixed and incubated at 37 °C. After that, Na_2CO_3 (0.06 mol L^{-1}) was added into the mixture to stop the reaction (total volume: 70 μL) at different reaction times (0–180 min). Finally, Glucose kit was used to detect the glucose content of the reaction. For maltase/CDs hybrids, maltase was substituted by maltase/LCDs or maltase/DCDs hybrids during the reaction. The inhibition ratio could be calculated by the following equation

$$\text{Inhibition ratio} = \frac{C_{\text{control}} - C_{\text{sample}}}{C_{\text{control}}} \times 100\% \quad (1)$$

Herein, C_{control} and C_{sample} denote the glucose content of the enzymatic reaction with maltase and maltase/CDs hybrids.

The Analysis of Michaelis–Menten Equation for Maltase: The analysis of Michaelis–Menten equation was carried out by the same method which reported by Li et al.^[30] In brief, a series concentration of substrate reacted with maltase or maltase/CDs hybrids and the initial reaction velocity of different concentration of maltose was obtained. Through plotting the $1/V$ (the reciprocal of initial reaction velocity) versus $1/[S]$ (the reciprocal of the concentration of substrate) to make a Lineweaver–Burk plot, where the ordinate intercept represents $1/V_{\max}$ and the abscissa intercept is the value of $-1/K_m$. Finally, the value of V_{\max} and K_m were obtained.

SDS-Polyacrylamide Gel Electrophoresis: The maltase and maltase/CDs hybrids (the concentration of maltase and LCDs or DCDs were 2.5 and 1.5 mg mL⁻¹) were separated by SDS-polyacrylamide gel electrophoresis (w/w: 8%), which contained lithium dodecyl sulfate (LDS, 1%) and β -mercaptoethanol (1%) in the sample loading buffer. The parameters were 80 V for 2 h. After that, Coomassie Brilliant Blue R-250 (0.25%) was used for staining the gel.^[35]

Cytotoxicity Analysis: The 293T cell line was used for evaluating the cytotoxicity of LCDs and DCDs. The 293T cells were incubated at 37 °C in 5% CO₂ for 24 h in 96-well plate. Then, a series concentration of CDs was added into 96-well plate. After 24 h, the viabilities of cells treated with different concentration of CDs was detect by Cell Counting Kit-8.

Statistical Analysis: The activity of maltase or maltase/LCDs or maltase/DCDs hybrids and the viability of 293T cells treated with chiral CDs were detected in triplicate. This data were presented as mean \pm standard deviation (SD). Statistical analysis of this results were utilized Independent-Samples T Test by GraphPad Prism 5.

Characterization: TEM images and HRTEM of chiral CDs were obtained by a transmission electron microscope with the accelerating voltage of 200 kV (Tecnaï G2 F20, FEI Corporation, American). AFM measurements of chiral CDs were conducted by a force microscope (Multimode V, Veeco Corporation, American). The XPS of chiral CDs were carried out with an X-ray photoelectron spectroscope (Ultra DLD, Shimadzu Corporation, Japan). FT-IR spectrum of chiral CDs and L- or D-Glu were obtained with a FT-IR spectrometer (Hyperion, Bruker Corporation, Germany). PL measurement of chiral CDs, maltase, and maltase/LCDs or maltase/DCDs hybrids were measured by a fluorescence spectrophotometer (Fluoromax-4, Jobin Yvon Company, France). The UV–vis absorption spectrum of chiral CDs was obtained with a UV–vis spectrophotometer (Evolution 220, Thermo, American). The hydrodynamic diameter of maltase and maltase/CDs hybrids were measured using a DLS instrument (Nano ZS90, Malvern Company, England). CD spectrum of chiral CDs, maltase, and maltase/CDs hybrids were recorded on a circular dichroism spectrometer (J-815, JASCO, Japan).

Supporting Information

Supporting Information is available from the Wiley Online Library or from the author.

Acknowledgements

This work was supported by National MCF Energy R&D Program (2018YFE0306105), the National Natural Science Foundation of China (51725204, 51572179, 21771132, 21471106), the Natural Science Foundation of Jiangsu Province (BK20161216), Collaborative Innovation Center of Suzhou Nano Science & Technology, the Priority Academic Program Development of Jiangsu Higher Education Institutions (PAPD), and the 111 Project.

Conflict of Interest

The authors declare no conflict of interest.

Keywords

carbon dots, chirality regulation, maltose enzyme activity, α -glucosidase inhibitors

Received: March 23, 2019

Revised: April 23, 2019

Published online:

- [1] S. E. Inzucchi, R. M. Bergenstal, J. B. Buse, M. Diamant, E. Ferrannini, M. Nauck, A. L. Peters, A. Tsapas, R. Wender, D. R. Matthews, *Diabetes Care* **2012**, *35*, 1364.
- [2] G. E. Umpierrez, F. J. Pasquel, *Diabetes Care* **2017**, *40*, 509.
- [3] J. L. Chiasson, R. G. Josse, M. Gomis, M. Hanefeld, A. Karasik, M. Laakso, S. N. T. R. Grp, *JAMA, J. Am. Med. Assoc.* **2003**, *290*, 486.
- [4] K. Borch-Johnsen, A. Neil, B. Balkau, S. Larsen, K. Borch-Johnsen, A. Nissinen, J. Pekkanen, J. Tuomilehto, S. Keinanen-Kiukkaanniemi, L. Hiltunen, S. L. Kivela, J. Tuomilehto, P. Lindstrom, J. Pyorala, M. Pyorala, K. Balkau, B. Eschwege, E. Gallus, G. Garancini, M. P. Schranz, A. Jousilahti, R. J. Heine, J. M. Dekker, E. Feskens, H. Lithell, B. Zethelius, M. Peltonen, N. Unwin, N. Ahmad, K. Alberti, M. M. Alberti, K. Borch-Johnsen, J. Eriksson, Q. Qiao, J. Tuomilehto, Q. Qiao, B. Balkau, T. J. uomilehto, Q. Qiao, K. Borch-Johnsen, B. Balkau, D. S. Grp, *Lancet* **1999**, *354*, 617.
- [5] S. E. Inzucchi, *JAMA, J. Am. Med. Assoc.* **2002**, *287*, 360.
- [6] D. M. Nathan, J. B. Buse, M. B. Davidson, E. Ferrannini, R. R. Holman, R. Sherwin, B. Zinman, *Diabetes Care* **2009**, *32*, 193.
- [7] S. Kumar, S. Narwal, V. Kumar, O. Prakash, *Pharmacogn. Rev.* **2011**, *5*, 19.
- [8] S. Y. Lim, W. Shen, Z. Q. Gao, *Chem. Soc. Rev.* **2015**, *44*, 362.
- [9] S. J. Zhu, Q. N. Meng, L. Wang, J. H. Zhang, Y. B. Song, H. Jin, K. Zhang, H. C. Sun, H. Y. Wang, B. Yang, *Angew. Chem., Int. Ed.* **2013**, *52*, 3953.
- [10] J. Du, N. Xu, J. Fan, W. Sun, X. Peng, *Small* **2019**, *15*, 1805087.
- [11] X.-W. Hua, Y. W. Bao, F. G. Wu, *ACS Appl. Mater. Interfaces* **2018**, *10*, 10664.
- [12] A. H. Loo, Z. Sofer, D. Bousa, P. Ulbrich, A. Bonanni, M. Pumera, *ACS Appl. Mater. Interfaces* **2016**, *8*, 1951.
- [13] H. Li, J. Huang, F. Lu, Y. Liu, Y. Song, Y. Sun, J. Zhong, H. Huang, Y. Wang, S. Li, *ACS Appl. Bio Mater.* **2018**, *1*, 663.
- [14] C. Viedma, *Phys. Rev. Lett.* **2005**, *94*, 065504.
- [15] L. D. Barron, *Space Sci. Rev.* **2008**, *135*, 187.
- [16] F. Li, Y. Li, X. Yang, X. Han, Y. Jiao, T. Wei, D. Yang, H. Xu, G. Nie, *Angew. Chem., Int. Ed.* **2018**, *57*, 2377.
- [17] R. Malishev, E. Arad, S. K. Bhunia, *Chem. Commun.* **2018**, *54*, 7762.
- [18] Q. Xin, Q. Liu, L. Geng, Q. Fang, J. R. Gong, *Adv. Healthcare Mater.* **2017**, *6*, 1601011.
- [19] L. Hu, H. Li, C. A. Liu, Y. Song, M. Zhang, H. Huang, Y. Liu, Z. Kang, *Nanoscale* **2018**, *10*, 2333.
- [20] S. Qu, D. Zhou, D. Li, W. Ji, P. Jing, D. Han, L. Liu, H. Zeng, D. Shen, *Adv. Mater.* **2016**, *28*, 3516.
- [21] W. Li, S. Wu, H. Zhang, X. Zhang, J. Zhuang, C. Hu, Y. Liu, B. Lei, L. Ma, X. Wang, *Adv. Funct. Mater.* **2018**, *28*, 1804004.
- [22] S. Bhattacharya, R. S. Phatake, S. Nabha Barnea, N. Zerby, J. J. Zhu, R. Shikler, N. G. Lemcoff, R. Jelinek, *ACS Nano* **2019**, *13*, 1433.
- [23] Y. Li, Y. Zhao, H. Cheng, Y. Hu, G. Shi, L. Dai, L. Qu, *J. Am. Chem. Soc.* **2012**, *134*, 15.
- [24] L. Dordevic, F. Arcudi, A. D'Urso, M. Cacioppo, N. Micali, T. Buergi, R. Purrello, M. Prato, *Nat. Commun.* **2018**, *9*, 3442.
- [25] H. Ming, Z. Ma, Y. Liu, K. Pan, H. Yu, F. Wang, Z. Kang, *Dalton Trans.* **2012**, *41*, 9526.

- [26] M. Zhang, L. Hu, H. Wang, Y. Song, Y. Liu, H. Li, M. Shao, H. Huang, Z. Kang, *Nanoscale* **2018**, *10*, 12734.
- [27] N. Suzuki, Y. Wang, P. Elvati, Z. B. Qu, K. Kim, S. Jiang, E. Baumeister, J. Lee, B. Yeom, J. H. Bahng, J. Lee, A. Violi, N. A. Kotov, *ACS Nano* **2016**, *10*, 1744.
- [28] M. Vazquez-Nakagawa, L. Rodriguez-Perez, M. A. Herranz, N. Martin, *Chem. Commun.* **2016**, *52*, 665.
- [29] M. Stumvoll, B. J. Goldstein, T. W. van Haefen, *Lancet* **2005**, *365*, 1333.
- [30] H. Li, S. Guo, C. Li, H. Huang, Y. Liu, Z. Kang, *ACS Appl. Mater. Interfaces* **2015**, *7*, 10004.
- [31] M. Dixon, *Biochem. J.* **1953**, *55*, 170.
- [32] A. V. Gusakov, A. P. Sinityn, *Biotechnol. Bioeng.* **1992**, *40*, 663.
- [33] B. A. Kikani, S. P. Singh, *Int. J. Biol. Macromol.* **2015**, *81*, 450.
- [34] W. C. Johnson, *Annu. Rev. Biophys. Biophys. Chem.* **1988**, *17*, 145.
- [35] H. Li, W. Kong, J. Liu, M. Yang, H. Huang, Y. Liu, Z. Kang, *J. Mater. Chem. B* **2014**, *2*, 5652.